Principal component analysis for feature extraction and NN pattern recognition in sensor monitoring of chip form during turning

T. Segreto [a,*], A. Simeone [b], R. Teti [a]

[a] Fraunhofer Joint Laboratory of Excellence on Advanced Production Technology, Department of Chemical, Materials and Industrial Production Engineering, University of Naples Federico II, Piazzale Tecchio 80, Naples 80123, Italy
[b] Centre for Sustainable Manufacturing and Reuse/Recycling Technologies Loughborough University, Leicestershire LE11 3TU, UK

A B S T R A C T

Experimental cutting tests on C45 carbon steel turning were performed for sensor fusion based monitoring of chip form through cutting force components and radial displacement measurement. A Principal Component Analysis algorithm was implemented to extract characteristic features from acquired sensor signals. A pattern recognition decision making support system was performed by inputting the extracted features into feed-forward back-propagation neural networks aimed at single chip form classification and favourable/unfavourable chip type identification. Different neural network training algorithms were adopted and a comparison was proposed.

© 2014 CIRP.

Introduction

The type and form of the produced chip is a critical aspect in machining processes, which strongly influences the cutting process stability: long chips can interfere with the machine tool, the workpiece and the tooling and have harmful impacts upon the material removal process and the product quality (Byrne et al., 1995; Jawahir and van Luttervelt, 1993; Santochi et al., 1997; Jemielniak and Otman, 1998; Barry and Byrne, 2002).

Small and broken chips are much simpler to handle, transfer, put in storage and recycle yielding positive environmental impacts on the manufacturing operations (Byrne et al., 2003; Santochi et al., 1997; Kim et al., 2005; Andreasen and De Chiffre, 1998; Viharos et al., 2003).

Machining processes which are likely to generate long and continuous chips, such as turning operations, can make the realization of an effectively functioning chip control a really difficult task because of the scarcity of guidelines and methods to forecast chip breakage and variations in chip breakability as a consequence of modifications in cutting conditions (Andreasen and De Chiffre, 1993, 1998; Segreto et al., 2005).

As a matter of fact, in the course of a metal cutting operation, process condition modifications arising from tool wear development, irregularity in work material properties, temperature related issues, etc., can generate significant alterations of the chip type and form with detrimental consequences on the manufacturing of the product. Accordingly, to prevent the formation of unfavourable chip types and damages to the machine, the tooling and the workpiece, sensor monitoring methods and chip form control are highly desirable (Segreto et al., 2009).

When measuring a particular variable of a manufacturing process, a single sensory data source for that variable may not be able to meet all the monitoring performance requirements. A solution to this problem is sensor fusion (Segreto and Teti, 2008) that combines multiple sensing units so that the resulting data information is more complete than when these data sources are used independently.

In this work, multiple digital signals obtained from sensor monitoring during turning of C45 carbon steel were employed for reliable chip form identification and monitoring (Teti et al., 2006a,b).

Sensor fusion paradigm through advanced signal processing, characterization and feature extraction based on the principal component analysis (PCA) algorithm (Krzanowski, 1988; Holland, 2008) was applied to the sensor signals (Simeone et al., 2013; Segreto et al., 2012a,b). The extracted significant features were used as input to cognitive decision making method based on neural network pattern recognition (Hertz et al., 1991; Segreto et al., 2013; D'Addona et al., 2011; Segreto and Teti, 2007) through the use of diverse training algorithm.

Materials and experimental procedures

An experimental campaign of turning tests under dry conditions (Fig. 1) was carried out on a carbon steel cylindrical

---

* Corresponding author. Tel.: +39 3471337695; fax: +39 0817682362.
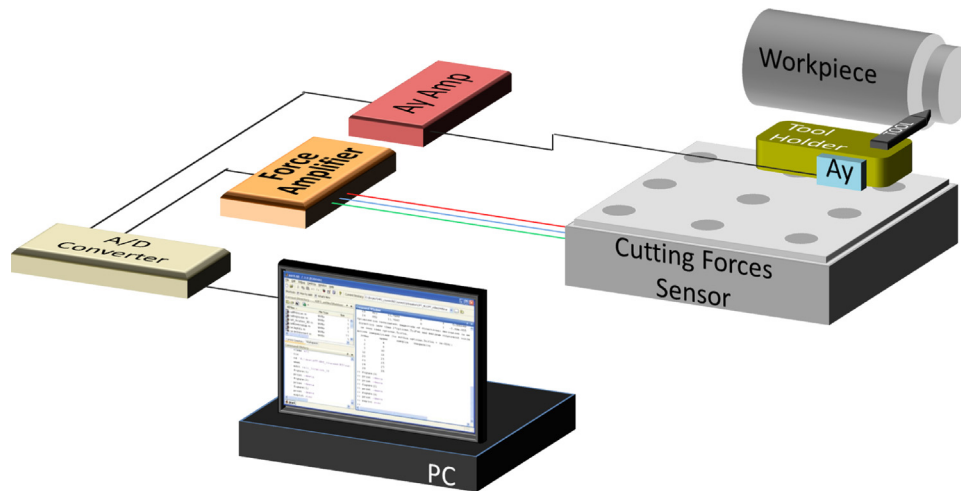 E-mail address: tsegreto@unina.it (T. Segreto).

Fig. 1. Experimental set-up general scheme.

rod by using a coated Kennametal tool insert (model TNMG332P KC 850), mounted on a standard SANDVIK tool holder (MTGNR/ L). The machine tool used for the cutting tests was a MAZAK CNC turning lathe (Model Quick Turn 10N).

Seven chip form types (ISO, 1993) were generated by varying the cutting parameters as shown in Fig. 2:

- snarled ribbon (1.3),
- long tubular (2.1),
- short tubular (2.2),
- long washer type helical (4.1),
- short washer type helical (4.2),
- connected arc (6.1),
- loose arc (6.2),

The following process parameters values were selected:

- Cutting speed, v_c = 150, 200, 250 m/min
- Feed rate, f = 0.1, 0.2, 0.3, 0.35, 0.4, 0.5 mm/rev
- Depth of cut, DoC = 1.0, 1.2, 1.3, 1.4, 1.5 mm

By combining the cutting parameters reported above, a total of 90 turning tests were performed and summarized in Table 1.

Advanced signal processing through principal components analysis

An advanced signal processing technique, based on the principal component analysis (PCA), also known as the

Table 1
Experimental turning test programme and related ISO chip form (v_c = cutting speed; DoC = depth of cut; f = feed rate, CF = chip form).

v_c (m/min)	DoC (mm)	f (mm/rev)	ID test	CF ISO	v_c (m/min)	DoC (mm)	f (mm/rev)	ID Test	CF ISO	v_c (m/min)	DoC (mm)	f (mm/rev)	ID test	CF ISO
150	1.0	0.1	T1353	1.3	200	1.0	0.1	T1384	1.3	250	1.0	0.1	T1323	1.3
		0.2	T1354	2.1			0.2	T1385	4.1			0.2	T1324	4.1
		0.3	T1355	2.2			0.3	T1386	4.1			0.3	T1325	4.2
		0.35	T1356	4.1			0.35	T1387	4.1			0.35	T1326	4.2
		0.4	T1357	4.1			0.4	T1388	4.1			0.4	T1327	4.2
		0.5	T1358	4.1			0.5	T1389	4.2			0.5	T1328	4.2
	1.2	0.1	T1347	1.3		1.2	0.1	T1378	1.3		1.2	0.1	T1317	1.3
		0.2	T1348	2.2			0.2	T1379	4.1			0.2	T1318	4.2
		0.3	T1349	6.1			0.3	T1380	2.2			0.3	T1319	2.2
		0.35	T1350	6.1			0.35	T1381	2.2			0.35	T1320	6.2
		0.4	T1351	6.1			0.4	T1382	2.2			0.4	T1321	6.2
		0.5	T1352	6.1			0.5	T1383	2.2			0.5	T1322	6.2
	1.3	0.1	T1341	1.3		1.3	0.1	T1372	1.3		1.3	0.1	T1311	1.3
		0.2	T1342	2.2			0.2	T1373	4.1			0.2	T1312	4.1
		0.3	T1343	6.1			0.3	T1374	6.2			0.3	T1313	2.2
		0.35	T1344	6.1			0.35	T1375	6.2			0.35	T1314	6.2
		0.4	T1345	6.2			0.4	T1376	6.2			0.4	T1315	6.2
		0.5	T1346	6.2			0.5	T1377	6.2			0.5	T1316	6.2
	1.4	0.1	T1335	1.3		1.4	0.1	T1366	1.3		1.4	0.1	T1305	1.3
		0.2	T1336	2.2			0.2	T1367	4.1			0.2	T1306	4.1
		0.3	T1337	6.1			0.3	T1368	6.2			0.3	T1307	6.2
		0.35	T1338	6.1			0.35	T1369	6.2			0.35	T1308	6.2
		0.4	T1339	6.1			0.4	T1370	6.2			0.4	T1309	6.2
		0.5	T1340	6.2			0.5	T1371	6.2			0.5	T1310	6.2
	1.5	0.1	T1329	1.3		1.5	0.1	T1360	1.3		1.5	0.1	T1157	1.3
		0.2	T1330	2.2			0.2	T1361	4.1			0.2	T1158	4.1
		0.3	T1331	6.1			0.3	T1362	6.2			0.3	T1301	6.2
		0.35	T1332	6.1			0.35	T1363	6.2			0.35	T1302	6.2
		0.4	T1333	6.1			0.4	T1364	6.2			0.4	T1303	6.2
		0.5	T1334	6.1			0.5	T1365	6.2			0.5	T1304	6.2
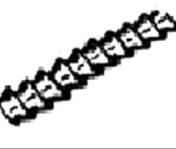
Cutting		Favourable	Unfavourable	
Straight	1 Ribbon Chips	1.2 Short		1.1 Long/1.3 Snarled
Mainly up curling	2 Tubular Chips	2.2 Short	2.1 Long	2.3 Snarled
	3 Spiral Chips		3.1 Flat/3.2 Conical	
Mainly Side curling	4 Washer type Chips	4.2 Short	4.1 Long	4.3 Snarled
Up and Side Curling	5 Conical Helical Chips	5.2 Short	5.1 Long	5.3 Snarled
	6 Arc Chips	6.2 Loose/6.1 Conn		
	7-8 Natural Broken Chips	7 Elemental		8 Needle

Fig. 2. Chip form classification (ISO 3685, 1993).

Karhunen–Loeve transformation (Holland, 2008), was implemented to the digital sensor signals detected during the experimental turning tests programme in order to obtain important characteristic signal features (Simeone et al., 2013; Segreto et al., 2012a,b).

The extraction of signal characteristic features from multiple sensing systems and the projection of complex multivariate data on lower dimensional spaces is of primary importance in many information processing fields such as pattern recognition, predictive modelling, industrial process fault diagnosis and control, etc. (Krzanowski, 1988).

PCA is a multivariate technique that analyzes a dataset in which observations are described by several inter-correlated quantitative dependent variables. Its goal is to extract the important information from the dataset, to represent it as a set of new orthogonal variables called principal components, and to display the pattern of similarity of the observations and of the variables as points in maps.

Principal component analysis basics

Assume that the output, X, from a multiple sensor system yielding a series of p sensor signals is a data matrix $n \times p$, where n = number of sensor signal samplings, with covariance matrix:

$$\Sigma_{ij} = cov(X_i, X_j) = E[(X_i - \mu_i)(X_j - \mu_j)] \tag{1}$$

where E is the expected value and $\mu_i = E(X_i)$ is the mean.

In PCA, a set of new variables is found which are uncorrelated and whose variance is maximized. These new variables, Y_i, are called the principal components and are related to the original variables, x_i, by:

$$Y_i = a_{i1} \times 1 + a_{i2} \times 2 + \cdots + a_{ip} x_p \tag{2}$$

The first principal component, Y_1, is found by setting $a_{11} \ldots a_{1n}$ so that the variance of Y_1 is maximized; the second principal component, Y_2, is found by choosing $a_{21} \ldots a_{2n}$ so that the variance of Y_2 is maximized for the data uncorrelated to Y_1; and so on.

Principal component analysis application

In the application reported in this paper, the extracted signal features consisted of the fused signals principal components variance values represented by the sensorial data "latent roots" obtained by PCA (Holland, 2008).

To implement PCA, data adjustment must be carried out by the mean centring of the data set. For this purpose, the mean of each variable was calculated and subtracted from the original data to generate a zero-mean distribution. Sensorial data matrices representing signals oscillating around zero (i.e. deprived of their continuous component and containing only frequency content information) are obtained to ensure that the first principal component describes the direction of maximum variance.

Each of the 90 experimental test cases is represented by a 8192×4 sensor fusion data matrix. The 4 columns correspond to the 4 original sensor signals variables (F_x, F_y, F_z and A_y) and the rows are the 8192 data samplings of the digital signals. This data matrix is the data set for the PCA based sensor fusion, as shown in Table 2 for test case T1353.

A covariance matrix along the 4 original variables (F_x, F_y, F_z and A_y) was evaluated from each sensor signals data matrix, generating a 4×4 matrix as shown in Table 3 for test case T1353. By repeating this calculation for all test cases, 90 covariance matrices were obtained.

From the covariance matrix of each test case, the eigenvectors matrix, A, was calculated. The matrix A elements, a_{ij}, called "loadings", are obtained under the constraint:

$$a_{11}^2 + a_{12}^2 + a_{13}^2 + a_{14}^2 = 1 \tag{3}$$

Table 2
Sensor fusion data matrix for test case T1353.

Samples	F_x	F_y	F_z	A_y
1	−53.1372	−12.9189	−15.3205	0.1000
...	...	...	...	...
8192	39.6362	26.1436	−4.3342	−0.0257

Table 3
Covariance matrix for test case T1353.

1023.1818	274.6762	413.6524	−0.3982
274.6762	271.1657	198.0914	−0.2271
413.6524	198.0914	344.1910	−0.1815
−0.3982	−0.2271	−0.1815	0.0027

Table 4
Eigenvectors matrix A for test case T1353.

Original variables	Principal components (new variables)			
	1st	2nd	3rd	4th
F_x	0.8548	−0.4950	−0.1559	−0.0003
F_y	0.3023	0.7191	−0.6258	−0.0007
F_z	0.4218	0.4878	0.7643	0.0002
A_y	−0.0004	−0.0003	0.0007	−1.0000

Table 5
Eigenvalues and explained variance for test case T1353.

Principal components	Eigenvalues (latent roots)	% Variance	% Cumulate
1st	1324.4228	80.8294	80.8294
2nd	216.4746	13.2114	94.0408
3rd	97.6414	5.9590	99.9999
4th	0.0024	0.0001	100.0000

Each row of matrix A represents one eigenvector and each column contains the loadings (relationship weights) of each new variable (principal component) on each original variable (sensor signal). In Table 4, the eigenvectors matrix A for test case T1353 is reported.

The eigenvectors define the directions of a new coordinate system where the coordinates of the data points of each test case are given by linear combinations of the original coordinates and the loadings (weights) a_{ij}. The new positions of the data points in the new system are called "scores".

Finally, the eigenvalues for each covariance matrix, also known as "latent roots", were then calculated. The latent roots for test case T1353 are shown in Table 5.

The evaluation of the covariance matrix eigenvalues was used as a criterion for selecting the number of principal components, according to (Cattell, 1966). The latent roots represent the amount of variance explained by each principal component and are required to decrease monotonically from first to last principal component. The latent roots for test case T1353 are plotted in the scree plot shown in Fig. 3: they explain the highest variance along the 1st principal component axis, which then decreases from the 2nd to the 4th principal component axis were it becomes extremely low.

Fig. 4 shows the biplot of the first 3 principal components axes. The biplot is a type of exploratory graph that allows information on both data samples and variables of a data matrix to be displayed graphically: data samples are displayed as points and variables as vectors (Greenacre, 2010).
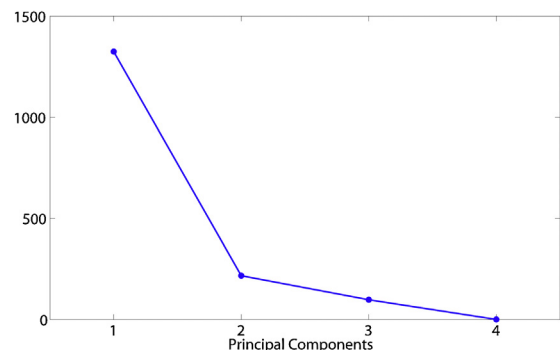

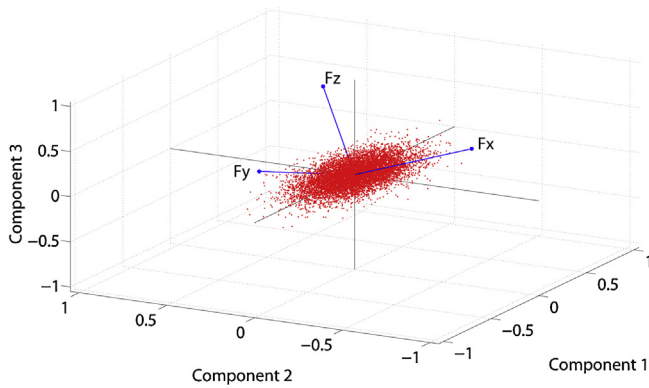**Fig. 3.** Test case T1353: eigenvalues scree plot.

Fig. 4. Test case T1353: biplot of the first 3 principal components axes; the PCA scores are displayed as red data points; the original variables F_x, F_y, F_z are displayed as blue vectors.

In the biplot of Fig. 4, the scores (data points in the new coordinate system) are displayed as red points and the original variables (sensor signals) are displayed as blue vectors.

The biplot shows that sensor signals F_x, F_y and F_z (original variables) are approximately aligned with the 1st, 2nd and 3rd principal component axes, respectively, suggesting a good relationship between these sensor signals and the first three principal components (new variables). The A_y component is too small to be visualized in the biplot because it has a lower order of magnitude than the other variables, highlighting hence a smaller importance.

Neural network pattern recognition for chip form

Neural network (NN) pattern recognition based on sensor fusion features extracted through PCA was utilized for decision making on chip form categorisation under two classifying perspectives: single chip form classification and favourable/unfavourable chip type identification.

The 4 principal components, obtained through PCA application to all test cases data matrices, were strongly related to the F_x, F_y, F_z and A_y sensor signals, respectively. They supplied sensor fusion features to construct 4-element feature vectors. In order to verify the significance of the 4th principal component, also 3-element feature vectors were built using the first 3 principal components (related to F_x, F_y, F_z) and excluding the forth one (related to A_y).

The two sets of feature vectors made up two different training sets for NN learning using diverse architectures for pattern recognition (Hertz et al., 1991; Jemielniak et al., 2006).

Data for classification problems are set up for a NN by organizing the data into two matrices, the input matrix and the target matrix. The input matrix is made of the 3- or 4-elements feature vectors (columns) and the 90 test cases (rows).

3-Layer feed-forward back-propagation NN (Fig. 5) were built with the following architecture: input layer with a number of nodes equal to the number of input signal feature (SF) vector elements; hidden layer with a number of nodes equal to 16 or 32, for 4-elements feature vectors, and 12 or 24, for 3-elements feature vectors.
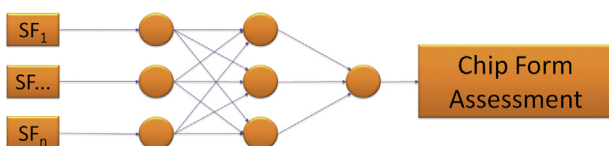

Fig. 5. Three layer feed-forward backpropagation neural network scheme for chip form identification.

Table 6
ISO-based chip form clusters and cluster elements.

Chip Form	ISO	Class
Continuous snarled	1.3	1
Long tubular chip	2.1	2
Long washer	4.1	
Short washer	4.2	3
Short tubular chip	2.2	
Connected arc	6.1	4
Loose arc	6.2	

In the case of single chip form classification, the seven ISO based types of produced chip forms were clustered into four classes, as reported in Table 6. For this purpose, the target vector contained one node, yielding a coded value associated to one chip form: 1 for the chip form cluster to be recognized and 0 for the other three chip form clusters. In this way, four different neural networks were built, each one aimed at discriminating one single chip form cluster.

In the case of favourable/unfavourable chip form identification, single chip forms were grouped into two clusters according to their being advantageous or disadvantageous:

- Favourable chip form cluster
- Chip form types 2.2, 4.2, 6.1, 6.2
- Unfavourable chip form cluster
- Chip form types 1.3, 2.1, 4.1

For this purpose, the NN target vector contains zeros for the favourable chip forms and ones for the unfavourable chip forms.

The node-configurations implemented on each neural network were: 4-16-1; 4-32-1; 3-12-1; 3-24-1.

Three different NN training algorithms were adopted for the chip form classification, as explained below.

Leave-k-out algorithm

The leave-k-out method (LKO), (Teti et al., 2006a) used for used for NN training and testing, was a supervised learning algorithm. In this procedure, one homogeneous group of k patterns (here, $k = 1$), extracted from the full training set, was held back in turn for testing and the rest of the patterns was used for training.

During testing, the NN output is correct if the actual output, O_a, is equal to the desired output, O_d, ±0.50% of the difference between adjacent chip form numerical codes, which was always 1.

By setting error $E = (O_a - O_d)$, the chip form identification is correct if $-0.5 \leq E \leq +0.5$; otherwise, a misclassification case occurs.

The ratio of correct classifications over total training cases yields the NN success rate (SR).

Levenberg –Marquardt algorithm

The Levenberg–Marquardt algorithm (Møller, 1993) was designed to approach second-order training speed excluding the Hessian matrix computation. When the performance function has the form of a sum of squares (as is typical in training feedforward networks), then the Hessian matrix can be approximated as

$$H = J^T J$$

and the gradient can be computed as

$$g = J^T e$$

where J is the Jacobian matrix that contains first derivatives of the network errors with respect to the weights and biases, and e is a vector of network errors. The Jacobian matrix can be computed through a standard back propagation technique that is much less complex than computing the Hessian matrix.

The Levenberg–Marquardt algorithm uses this approximation to the Hessian matrix in the following update:

$$X_{k+1} = X_k - [J^T J + \mu I]^{-1} J^T e$$

When the scalar μ is zero, this is just Newton's method, using the approximate Hessian matrix. When μ is large, this becomes gradient descent with a small step size. Thus, μ is decreased after each successful step (reduction in performance function) and is increased only when a tentative step would increase the performance function. In this way, the performance function will always be reduced at each iteration of the algorithm.

Scaled conjugate gradient algorithm

The scaled conjugate gradient backpropagation, developed by (Møller, 1993) is a supervised learning algorithm for feedforward neural networks that combines the model-trust region approach with the conjugate gradient approach. The basic back-propagation algorithm adjusts the weights in the steepest descent direction (negative of the gradient). This is the direction in which the performance function is decreasing most rapidly. It turns out that, although the function decreases most rapidly along the negative of the gradient, this does not necessarily produce the fastest convergence.

In the conjugate gradient algorithms, a search is performed along conjugate directions, which produces generally faster convergence than steepest descent directions.

For both LM algorithm and SCG algorithm data division for NN learning was carried out by randomly subdividing the initial data set into three sub-sets with the following percentages: 70% for training set; 15% for validation set; 15% for testing set.

The Training Set is the data set used for the NN training phase by adjusting the NN weights. The Validation Set is the data set used to minimize overfitting. No adjustment of the NN weights occurs with this data set, but only the verification that any increase in accuracy over the training data set actually yields an increase in accuracy over a data set that has not been shown to the network before. If the accuracy over the training data set increases, but the accuracy over the validation data set stays the same or decreases, then the NN is being overfitted and the training should be stopped. The Testing Set is a data set used only for testing the final solution in order to confirm the actual predictive power of the learned NN.

The validation performance of the NN was calculated by considering the Mean Squared Error (MSE), as shown in Fig. 6 for

Fig. 6. Neural network validation performance through MSE evaluation.

NN configuration 4-16-1. For every test case, the classification results are summarized in four confusion matrices, respectively the training, validation, testing and overall confusion matrix, as reported in Fig. 7.

Results and discussion

Table 7 report the NN pattern recognition success rate (SR) for single chip form classification (Class 1–4) and favourable/unfavourable (F/U) chip type identification using 4- and 3-element principal component related input feature vectors.

The comparison of the NN SR for favourable/unfavourable chip type identification with the averaged values of NN SR for single chip forms classification shows that there is no significant difference between the two approaches (Table 7). At times, the NN SR for favourable/unfavourable chip form is slightly higher than the NN SR for single chip forms and, at other times, the opposite is verified.

In all cases, moreover, the NN SR values are always higher than or equal to 80% confirming the capability of PCA in extracting valuable sensory features for chip form monitoring.

This result is somewhat unexpected because the two-classes (favourable/unfavourable chip forms) discrimination task is undoubtedly simpler than the four-classes (four single chip forms) recognition effort. However, if the single chip form identification NN SR are examined separately rather than as averaged values (Table 7), it can be noted that there are some, though very few, cases where the NN SR is lower than 70%, a situation never verified for the favourable/unfavourable that display NN SR always higher than 80%. This confirms that the four-classes classification task is actually a harder one especially by the Scaled Conjugate Gradient and the Leave-k-out algorithms.

As regards NN SR for single chip form classification, the snarled chip form cluster (Class 1) recognition shows NN SR values varying from 91% to 99%; for the long chip form cluster (Class 2) the success rate range decreases, with a minimum value of 77% and a maximum value of 91%; lower success rate values were obtained for the short chip form cluster (Class 3), from 60% to 91%; the loose chip form cluster (Class 4) shows a SR range varying from 71% up to 90%. The last two extremely variable ranges demonstrate that these chip form class (Class 3 and 4)are more difficult to be recognized than the others (Class 1 and 2).

Table 7 shows that the Levenberg–Marquardt training algorithm performs significantly better than the Scaled Conjugate Gradient and the Leave-k-out algorithms both for favourable/unfavourable chip form identification and for every single chip form classification. Moreover, the NN SR obtained with Levenberg–Marquardt algorithm is always >80% whereas with the Scaled Conjugate Gradient and the Leave-k-out algorithms it can be, though in few cases, <70% (Table 7).

The NN SR for the 4-input nodes NN configurations is generally, though slightly, higher than for the 3-input nodes feature vectors. This indicates that the sensor fusion of the diverse sensory data (cutting force components and one component response amplitude in radial direction) provides a synergic effect on the pattern recognition task, even if limited in magnitude.

The number of nodes at the hidden layer does not show a clear impact on the NN SR: the NN SR differences are either null or very reduced. In the latter cases, at times, the 4-input nodes NN configurations with higher number of hidden nodes have a higher NN SR whereas, at other times, this occurs for the 3-input nodes NN configurations.
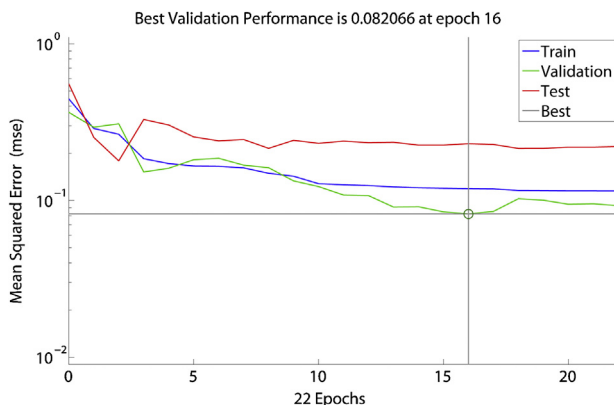
Test Confusion Matrix

52 83.9%	**1** 1.6%	98.1% 1.9%
0 0.0%	**9** 14.5%	100% 0.0%
100% 0.0%	90.0% 10.0%	98.4% 1.6%

Output Class / Target Class (0, 1)

All Confusion Matrix

13 92.9%	**0** 0.0%	100% 0.0%
0 0.0%	**1** 7.1%	100% 0.0%
100% 0.0%	100% 0.0%	100% 0.0%

Output Class / Target Class (0, 1)

Test Confusion Matrix

10 71.4%	**0** 0.0%	100% 0.0%
0 0.0%	**4** 28.6%	100% 0.0%
100% 0.0%	100% 0.0%	100% 0.0%

Output Class / Target Class (0, 1)

All Confusion Matrix

75 83.3%	**1** 1.1%	98.7% 1.3%
0 0.0%	**14** 15.6%	100% 0.0%
100% 0.0%	93.3% 6.7%	98.9% 1.1%

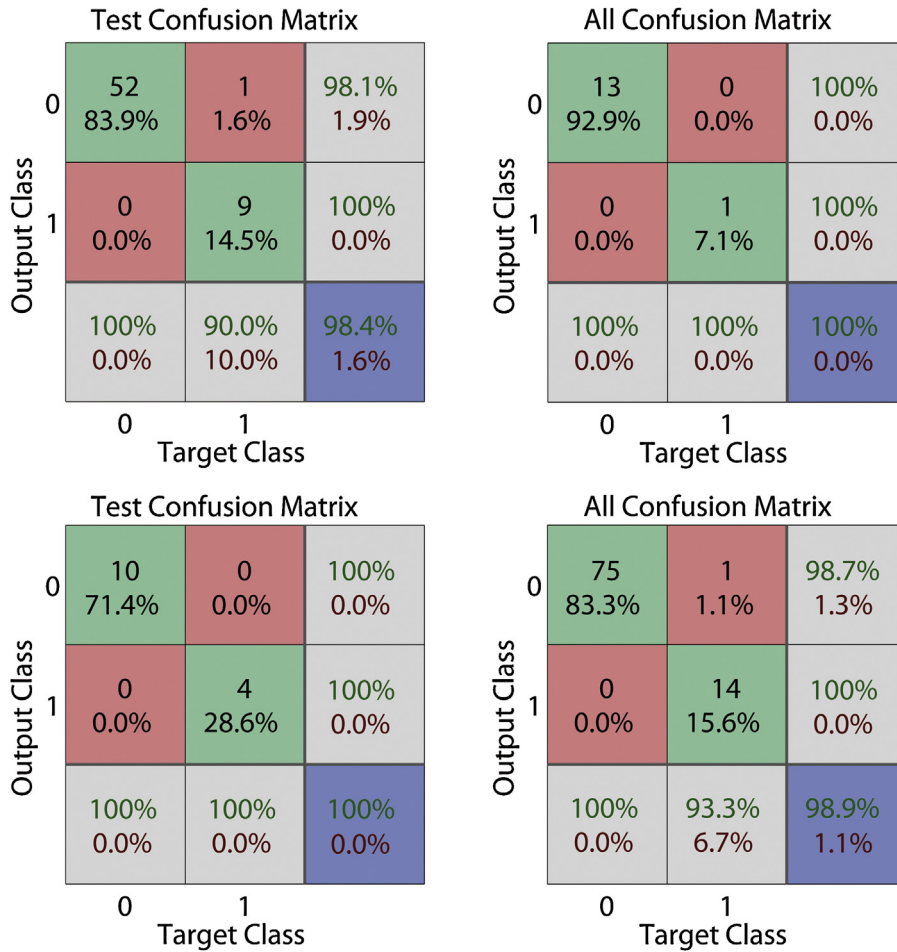Output Class / Target Class (0, 1)

Fig. 7. Confusion matrices for the 4-16-1 LM Class 1 NN configuration. The diagonal cells show the number of cases that were correctly classified and the off-diagonal cells show the misclassified cases. Blue cell in the bottom right: total % of correctly classified cases (in green) and the total % of misclassified cases (in red). (For interpretation of the references to color in this figure legend, the reader is referred to the web version of the article.)

Table 7
NN SR results for single chip form classification and favourable/unfavourable (F/U) chip form identification.

Training algorithm	NN Config.	Class 1	Class 2	Class 3	Class 4	Average SR (%)	F/U SR (%)
LM	4-16-1	99	91	84	88	91	92
	4-32-1	99	89	89	90	92	92
	3-12-1	99	89	91	84	91	87
	3-24-1	99	88	93	87	92	87
SCG	4-16-1	99	90	82	83	89	82
	4-32-1	99	91	82	84	89	88
	3-12-1	93	88	67	78	82	87
	3-24-1	97	88	60	77	81	84
LKO	4-16-1	92	83	77	81	83	83
	4-32-1	94	77	68	74	78	80
	3-12-1	93	80	82	71	82	82
	3-24-1	91	82	74	73	80	80

By implementing the principal components analysis (PCA), advanced signal processing, characterization and feature extraction were performed, and neural network based pattern recognition approach was adopted as decision making support system.

The NN success rates in chip form recognition were always higher than 80%, validating the capability of PCA in extracting valuable sensory features for chip form monitoring.

The 4 and 3 principal components, obtained through PCA application were utilized to construct input features vectors for feed-forward back-propagation neural network training with the use of three diverse learning algorithm: leave-k-out method (LKO), Levenberg–Marquardt (LM) algorithm, and Scaled Conjugate Gradient (SCG) algorithm.

The NN success rates (higher than 80%) obtained with the application of the three diverse algorithm show an efficient classification in chip form recognition. This is due to the capability of PCA in extracting valuable sensory features.

The favourable/unfavourable chip type identification yielded higher NN SR values than the single chip form classification, as a four classes (four chip forms) recognition effort is undoubtedly harder than a two-classes (favourable/unfavourable chip form) discrimination task.

The NN SR values for the 4-element feature vectors are higher than for the 3-element feature vectors cases, confirming that sensor fusion of sensorial data of different kinds can be positively valuable for pattern recognition.

Conclusions

Sensor fusion of digital signals acquired during sensor monitoring of longitudinal turning operations carried out on C45 carbon steel was detected with the aim to achieve the single chip form classification and favourable/unfavourable chip type identification.

By comparing the NN SR obtained for three diverse learning algorithm, the Levenberg–Marquardt (LM) is demonstrated to be the most suitable algorithm for pattern recognition decision making support system.

Acknowledgements

References

Andreasen, J.L., De Chiffre, L., 1993, Automatic Chip-Breaking Detection in Turning by Frequency Analysis of Cutting Force, CIRP Annals, 42/1: 45–48.

Andreasen, J.L., De Chiffre, L., 1998, An Automatic System for Elaboration of Chip Breaking Diagrams, CIRP Annals, 47/1: 35–40.

Barry, J., Byrne, G., 2002, Chip Formation, Acoustic Emission and Surface Layers in Hard Machining, CIRP Annals, 51/1: 65–70.

Byrne, G., Dornfeld, D., Inasaki, I., Ketteler, G., Koening, W., Teti, R., 1995, Tool Condition Monitoring: The Status of Research and Industrial Application, CIRP Annals, 44/2: 541–567.

Byrne, G., Dornfeld, D., Denkena, B., 2003, Advancing Cutting Technology, CIRP Annals, 52/2: 483–507.

Cattell, R.B., 1966, The Scree Test for the Number of Factors, Multivariate Behavioral Research, 1:245–276.

D'Addona, D., Segreto, T., Simeone, A., Teti, R., 2011, ANN Tool Wear Modelling in the Machining of Nickel Superalloy Industrial Products, CIRP Journal of Manufacturing Science and Technology, 4/1: 33–37.

Greenacre, M., 2010, Biplots in Practice, BBVA Foundat., Madrid.

Hertz, J., Krogh, A., Palmer, R.G., 1991, Introduction to the Theory of Neural Computation, Addison-Wesley, New York.

Holland, S.M., 2008, Principal Components Analysis (PCA), University of Georgia Press.

ISO 3685. 1993, Tool-Life Testing with Single-Point Turning Tools, Annex G, 41.

Jawahir, I.S., van Luttervelt, C.A., 1993, Recent Developments in Chip Control Research and applications, Annals of the CIRP, 42/2: 659–693.

Jemielniak, K., Otman, O., 1998, Catastrophic Tool Failure Detection Based on AE Signal Analysis, CIRP Annals, 47/1: 31–34.

Jemielniak, K., Teti, R., Kossakowska, J., Segreto, T., 2006, Innovative Signal Processing for Cutting Force Based Chip Form Prediction, Special Session on ICME (2nd Int. Virtual Conf. on Intelligent Production Machines and Systems – IPROMS 2006. 3–14 July), pp.7–12.

Kim, J.H., Chang, H.K., Han, D.C., Jang, D.Y., Oh, S.I., 2005, Cutting Force Estimation by Measuring Spindle Displacement in Milling Process, CIRP Annals, 54/1: 67–70.

Krzanowski, W.J., 1988, Principles of Multivariate Analysis: A User's Perspective, Oxford University Press, New York.

Møller, M.F., 1993, Neural Networks, 6:525–533.

Santochi, M., Dini, G., Tantussi, G., 1997, A Sensor-Integrated Tool for Cutting Force Monitoring, CIRP Annals, 46/1: 49–52.

Segreto, T., Andreasen, J.L., De Chiffre, L., Teti, R., 2005, Chip Form Monitoring in Turning Based on Neural Network Processing of Cutting Force Sensor Data, 1st I PROMS Virtual International Conference on Intelligent Production Machines and Systems (IPROMS 2005, 4–15 July), pp.609–614.

Segreto, T., Teti, T., 2007, Tool Condition Monitoring in Composite Materials Machining through Neural Network Processing of Acoustic Emission, 3rd IPROMS Virtual International Conference on Intelligent Production Machines and Systems (IPROMS 2007, 2–13 July), pp.642–647.

Segreto, T., Teti, R., 2008, Sensor Fusion of Acoustic Emission and Cutting Force for Tool Wear Monitoring during Composite Materials Machining, 6th CIRP Int. Conf. on Intelligent Computation in Manufacturing Engineering (CIRP ICME '08, Naples, 23–25 July), pp.216–221.

Segreto, T., Teti, R., Neugebauer, R., Schmidt, G., 2009, Shape Memory Alloy Machining Evaluation through Cutting Force Sensor Monitoring, 5th I*PROMS NoE Virtual Int. Conf. on Innovative Production Machines and Systems (IPROMS 2009, 6–17 July), pp.47–52.

Segreto, T., Simeone, A., Teti, R., 2012, Sensor Fusion for Tool State Classification in Nickel Superalloy High Performance Cutting, 5th CIRP International Conference on High Performance Cutting (Procedia CIRP, 1), pp.593–598.

Segreto, T., Simeone, A., Teti, R., 2012, Chip Form Classification in Carbon Steel Turning through Cutting Force Measurement and Principal Components Analysis (1st CIRP Global Web Conference: Interdisciplinary Research in Production Engineering (CIRPe 2012). Procedia CIRP, 2), pp.49–54.

Segreto, T., Simeone, A., Teti, R., 2013, Multiple Sensor Monitoring in Nickel Alloy Turning for Tool Wear Assessment via Sensor Fusion (8th CIRP Conference on Intelligent Computation in Manufacturing Engineering, Procedia CIRP, 12), pp.85–90.

Simeone, A., Segreto, T., Teti, R., 2013, Residual Stress Condition Monitoring via Sensor Fusion in Turning of Inconel 718 (8th CIRP Conference on Intelligent Computation in Manufacturing Engineering, Procedia CIRP, 12), pp.67–72.

Teti, R., Jawahir, I.S., Jemielniak, K., Segreto, T., Chen, S., Kossakowska, J., 2006, Chip Form Monitoring through Advanced Processing of Cutting Force Sensor Signals, CIRP Annals, 55/1: 75–80.

Teti, R., Jawahir, I.S., Segreto, T., Chen, S., 2006, Cutting Force Signal Pattern Recognition for Chip Form Identification (Proceedings of 5th CIRP Int. Sem. on Intelligent Computation in Manufacturing Engineering CIRP ICME'06, Ischia, 25–28 July), pp.685–690.

Viharos, Z.J.m, Markos, S., Szekeres, C., 2003, ANN-Based Chip-Form Classification in Turning (Proc. of the XVII IMEKO World Congress, June 22–27, Dubrovnik), pp.1469–1473.